Nanotechnology for Environmental Engineering (2025) 10:33
https://doi.org/10.1007/s41204-025-00439-3

ORIGINAL PAPER

Performance and emission analysis of diesel engine operating with hybrid nanoparticles dispersed *Madhuca longifolia* biodiesel

Balaji Ashok Kumar Bylapudi[1] · Venkata Subbaiah Kambagowni[1] · Jaikumar Sagari[2]

Received: 16 May 2024 / Accepted: 21 April 2025 / Published online: 30 April 2025

Abstract
This study investigates the performance and emissions of a single-cylinder diesel engine fueled with a ternary fuel mixture of hybrid nanoparticles such as ferric chloride ($FeCl_3$) and graphene. The fuel mixture consists of 70% diesel, 20% *Madhuca longifolia* biodiesel and 10% ethanol. Hybrid nanoparticles at concentrations of 50 and 75 mg/L were added to the ternary fuel mixture, with Cetyltrimethylammonium Bromide (CTAB) and QPAN added in a 1:1 ratio to increase the stability of the nanoparticles. The stability was measured according to the principle of photo spectroscopy and the fuel properties were evaluated according to American Society for Testing and Materials (ASTM) standards. The experimental methodology included varying the injection pressures to 200, 225, and 250 bars, along with different loads of 3, 6, 9, and 12 kgf, in a diesel engine to evaluate its performance and emission characteristics. The results showed that the addition of nanoparticles led to an improvement in brake thermal efficiency (BTE) and a reduction in brake specific fuel consumption (BSFC) as well as a reduction in carbon monoxide (CO), unburnt hydrocarbons (UHC), oxides of nitrogen (NO_x), and smoke opacity compared to diesel and ternary fuel blend. Of all the fuel samples, D70B20E10NPs75 mg/L QPAN75 mg/L performed best, achieving a BTE of 33.26% and a BSFC of 0.206 kg/kWh, while CO, UHC, NO_x, and smoke opacity at an injection pressure of 250 bar were 0.019%, 21 ppm, 833 ppm, and 36.25% respectively.

Keywords Ternary fuel blend · Brake specific fuel consumption · Cetane index · Ethanol · Carbon monoxide

Abbreviations

D100	Pure diesel
D70B20E10	70% diesel + 20% biodiesel + 10% ethanol
D70B20E10NPs50 mg/L	70% diesel + 20% biodiesel + 10% ethanol + 50 mg/L hybrid nanoparticles
D70B20E10NPs75 mg/L	70% diesel + 20% biodiesel + 10% ethanol + mg/L hybrid nanoparticles
D70B20E10NPs50CTAB50 mg/L	70% diesel + 20% biodiesel + 10% ethanol + 50 mg/L hybrid nanoparticles CTAB 50 mg/L
D70B20E10NPs75CTAB75 mg/L	70% diesel + 20% biodiesel + 10% ethanol + 50 mg/L hybrid nanoparticles + CTAB 75 mg/L
D70B20E10NPs50QPAN50 mg/L	70% diesel + 20% biodiesel + 10% ethanol + 50 mg/L hybrid nanoparticles + QPAN 50 mg/L
D70B20E10NPs75QPAN75 mg/L	70% diesel + 20% biodiesel + 10% ethanol + 50 mg/L hybrid nanoparticles + QPAN 75 mg/L
NaOH	Sodium hydroxide
Al_2O_3	Aluminum oxide

✉ Jaikumar Sagari
sagari.jaikumar1@gmail.com

[1] Department of Mechanical Engineering, Andhra University, Visakhapatnam, India

[2] School of Marine Engineering and Technology, Indian Maritime University, Kolkata, India

NPs	Nanoparticles (hybrid nanoparticles of $FeCl_3$ and graohene)
BTE	Brake thermal Efficiency (%)
BSFC	Brake specific fuel consumption (kg/kWh)
CO	Carbon monoxide (%)
UHC	Un burnt hydrocarbons (ppm)
NO_x	Oxides of nitrogen (ppm)
ppm	Part per million
ASTM	American standards for testing materials
SEM	Scanning electron microscope
XRD	X-Ray diffraction
$FeCl_3$	Ferric chloride
RSM	Response surface methodology
IP	Injection pressure (bar)

Introduction

As urbanization increases around the world, so does the need to reduce the amount of pollutants released into the environment, particularly in the transport sector. A nation's economic standing is influenced by a number of key factors, including the ease with which energy can be generated and converted. In contrast to other methods of energy conversion, compression ignition engines are characterized by a number of features [1–3]. In view of the depletion of conventional energy sources and the high pollutant emissions of combustion engines, the transition to sustainable fuels is becoming increasingly important. Researchers are actively exploring innovative approaches to minimize fuel consumption and emissions [4, 5]. Biodiesel has emerged as a promising and environmentally friendly alternative for internal combustion engines, offering the potential to increase performance while reducing emissions. Its inherent oxygen content improves combustion efficiency, resulting in lower pollutant emissions compared to conventional diesel. While numerous studies confirm that biodiesel reduces exhaust emissions, its impact on engine performance remains marginal [6, 7]. Another shortcoming of biodiesel is the increase in oxides of nitrogen (NO_x) emissions. Gaseous fuels, alcohols and nanoparticles can be added to reduce emissions and improve performance [8, 9]. A promising future development for the use of diesel engines is the possibility of improving the fuel properties of nanofuel by increasing the dispersion of nanoparticles in diesel/biodiesel blends. Carbon nanotubes, metal oxides, ferrous, and inorganic materials are among the possible sources of nanofuels. The oxidation of metal particles can generate more heat than conventional diesel and biodiesel fuels combined, but has a major stability disadvantage. However, there are a number of ways to mitigate this disadvantage [10–12]. Simhadri et al. [13] experimented with titanium dioxide (TiO_2) nanoparticles on Mahua biodiesel. They noticed an improvement in combustion and performance as well as a reduction in pollutants. Garugubilli et al. [14] investigated how copper oxide (CuO) nanoparticles and *Azadirachta indica* biodiesel. They reported that the brake thermal efficiency (BTE), brake specific fuel consumption (BSFC), cylinder pressure (CP), and net heat release rate (NHRR) were improved while the emissions of carbon monoxide (CO), unburnt hydrocarbons (UHC), NO_x, and smoke were reduced. Kunchi et al. [15] discovered the use of multi-ferrite nanoparticles for *Terminalia bellirica* biodiesel. According to the study, both performance and combustion indices were improved. In addition, a remarkable reduction in pollutant levels was observed compared to the emissions of standard diesel fuel. Kari et al. [16] studied the impact of chromium oxide (Cr_2O_3) nanoparticles on *Mesua ferrea* biodiesel using both experimental and theoretical methods. The researchers found that the actual performance of the experiment closely matched the predicted results indicated by the response surface methodology (RSM). Ansari et al. [17] studied the role of Jatropha biofuel and aluminum oxide (Al_2O_3) nanoparticles on diesel engine. The researchers found that biodiesel with nanoparticles worked better than regular fuel and produced fewer emissions. Janakiraman et al. [18] explored the role of TiO_2 nanoparticles in ternary mixes of diesel, biodiesel, and bioethanol in a diesel engine. The research discovered that the BTE reduced as compared to mineral diesel, while the brake specific energy consumption (BSEC) enhanced. The research also revealed a considerable drop in UHC and CO emissions, although NO_x increased.

Since ternary fuel blends can be used instead of regular diesel, they have recently gained enormous popularity worldwide. One important oxygenated source is ethanol, a sustainable fuel. However, it cannot be used as the main fuel source for diesel engines. In addition, this fuel is blended in varying proportions with diesel or biodiesel for further use. Diesel fuel is poorly soluble in ethanol, so an intermediate product such as biodiesel must be used for blending. The stable mixture that forms is created by the biodiesel dispersing the ethanol particles in the diesel fuel. Nevertheless,

Table 1 Details of materials and chemicals

Product	Company name	City/Town	Country
M. longifolia oil	Sivaroma Naturals Pvt. Ltd	Noida, Uttar Pradesh	India
Ferric chloride ($FeCl_3$) and graphene nanoparticles	Nano Research Lab (NRL)	Jamshedpur, Jharkhand	India
CTAB and QPAN 80	Otto Chemie Pvt. Ltd.	Sativali, Maharashtra	India
NaOH, Hexane, ethanol, methanol, and other chemicals	Vizag chemicals international	Visakhapatnam	India

biodiesel must be used as an intermediate in diesel engines in order to run on ethanol [11, 19, 20].

Denbratt et al. [21] investigated the effects of various higher alcohol types added to engines on their exhaust and combustion properties. Their results showed a significant reduction in CO and smoke compared to diesel. It was also found that the blends had a higher BSFC. Yesilyurt et al. [22] investigated how various parameters of diesel engines are affected by safflower-diesel blends. According to their results, the use of a ternary fuel blend lowered the BSFC while increasing the BTE. Furthermore, emissions were minimized by the addition of pentanol. Yilmaz et al. [23]. conducted an emissions test with a ternary blend whose ethanol content was gradually increased. The researchers found that higher ethanol concentrations led to lower emissions. At high and medium loads, in addition to the reduction in NO_x emissions, there was also a notable reduction in HC and CO. The effectiveness of diesel/biodiesel blends containing oxygenated alcohols and fuel additives in the form of nanoparticles was investigated in diesel engines by Mujtaba et al. [24]. It was found that alcohols and B30 reduced NO_x emissions, while carbon nanotubes (CNTs) and B30 reduced CO and HC emissions.

Previous studies have shown that while biofuels and alcohol additives in combination with nanoparticles contribute significantly to reducing emissions, the use of fossil fuels in diesel engines leads to environmental pollution. Therefore, the aim of this work was to investigate the effects of hybrid nanoparticles of ferric chloride ($FeCl_3$) and graphene in a ternary fuel blend on the evaluation of diesel engine performance and emission characteristics by varying injection pressure and load. The combination of hybrid nanoparticles and ternary fuel mixture in diesel engines is a completely new approach.

Materials and methods

Materials

The crude *Madhuca longifolia* oil was obtained from local traders. The chemicals such as methanol, sodium hydroxide (NaOH), hexane, surfactant (CTAB), dispersant (QPAN 80), $FeCl_3$ nanoparticles, graphene nanoparticles, and ethanol were procured from various chemical laboratories/vendors. All chemicals were procured with a purity of 99.99%. The details of all the chemicals/materials were presented in Table 1.

Transesterification process

Figure 1 shows the graphical representation of biodiesel production. The transesterification process was used to produce biodiesel from *M. longifolia*. Crude *M. longifolia* oil was heated to 50oC in a beaker. It was then combined with a

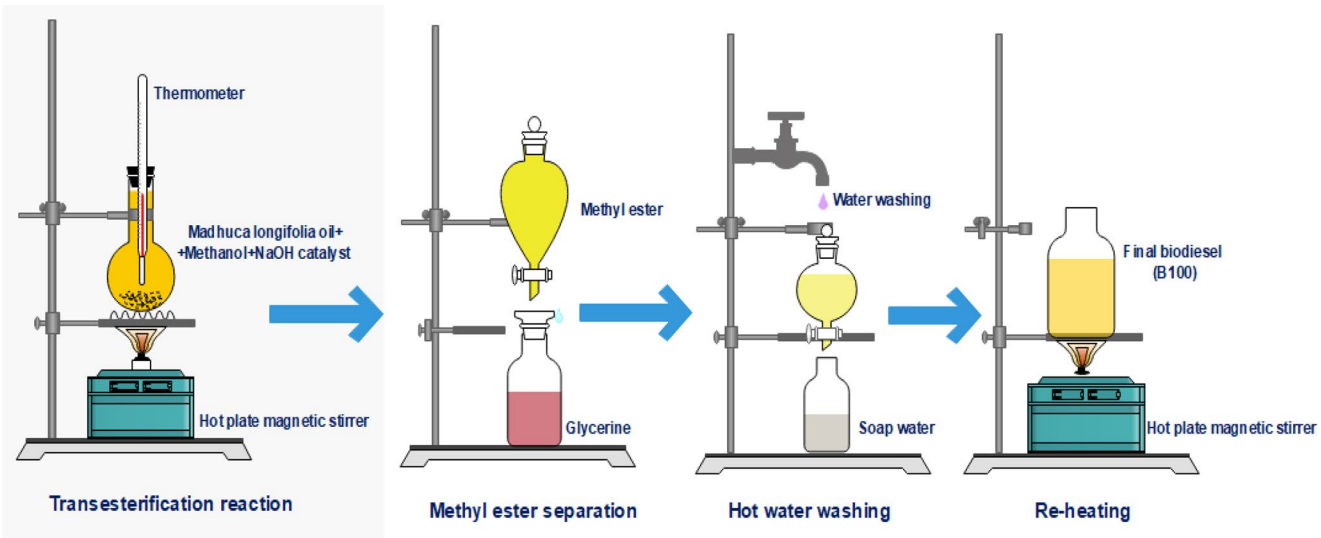

Fig. 1 Biodiesel preparation using transesterification process

NaOH catalyst and methanol. The magnetic stirrer ensured better mixing of the mixture so that a state of equilibrium was reached. The process lasted one hour at 60 °C. After the chemical reaction, glycerol and methyl ester were separated using a separating funnel. The methyl ester was then washed and heated again to remove the moisture it contained. The yield of biodiesel was determined using Eq. (1), and the calculated yield was 98%.

$$\text{Biodiesel yield } (\%) = \left(\frac{\text{Weight of biodiesel produced}}{\text{Weight of oil used}}\right) \times 100 \quad (1)$$

Nanoparticles characterization

XRD characterization was performed separately for $FeCl_3$ and graphene oxide nanoparticles. The XRD pattern of $FeCl_3$ nanoparticles is shown in Fig. 2(a), while Fig. 2(b)

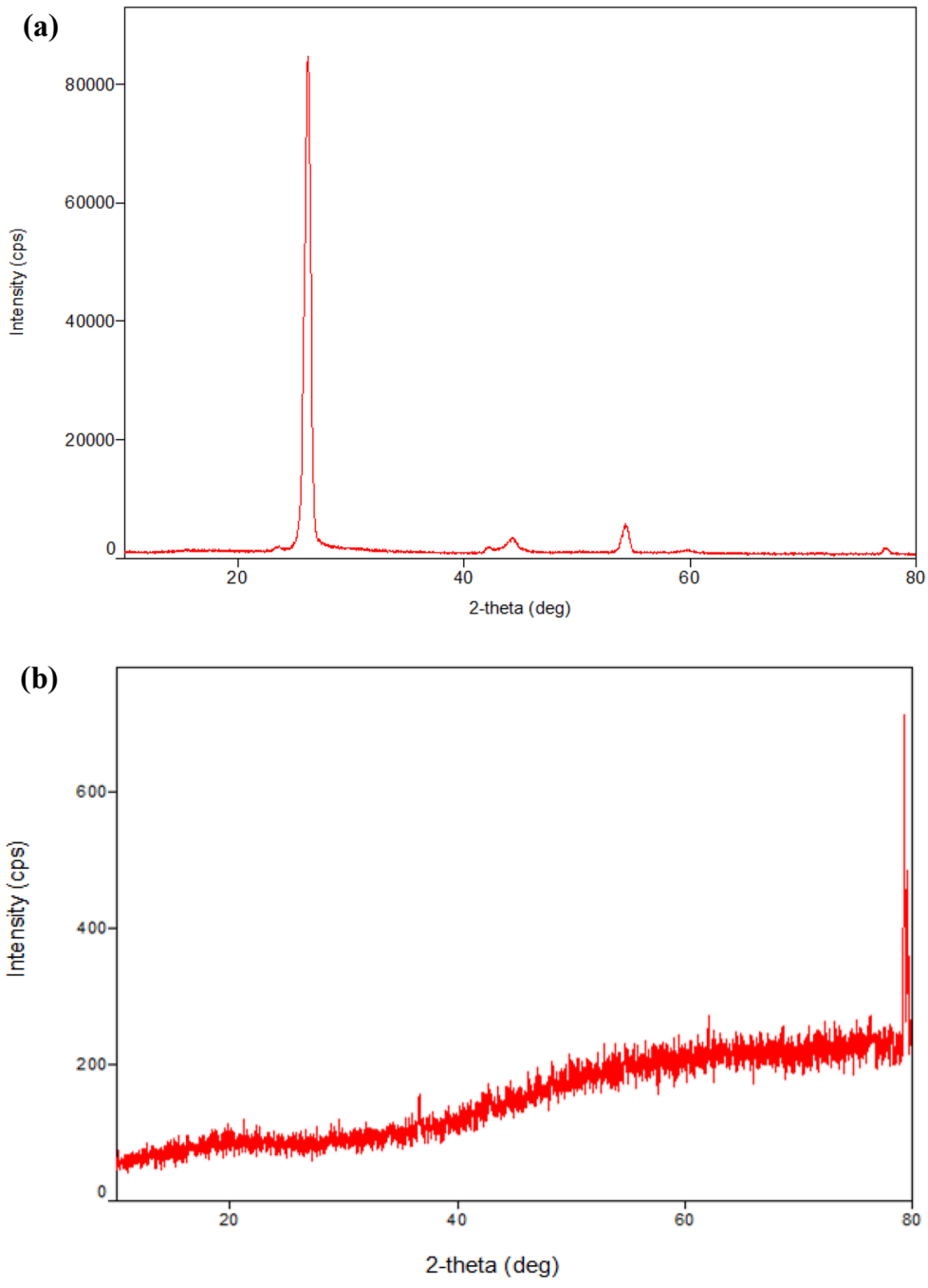

Fig. 2 **(a)** XRD patterns of graphene oxide nano powder. **(b)** XRD patterns of zinc oxide nano powder

shows the pattern for graphene oxide. In Fig. 2(a), a prominent peak at 2θ = 79.28° can be seen, along with several smaller peaks, confirming the hexagonal crystal structure of $FeCl_3$ nanoparticles with an interplanar spacing of d = 1.207 Å. In contrast, Fig. 2(b) shows a sharp and well-defined peak at 2θ = 26.23°, which is characteristic of the graphitic crystal structure with an interlayer spacing of d = 3.3947 Å.

The average crystallite sizes of graphene oxide and $FeCl_3$ nanoparticles were determined from XRD data using the Scherrer equation: $D = K\lambda / \beta \cos\theta$, where D represents the particle size, K is the shape factor, λ is the wavelength of the incident X-ray beam, θ is the Bragg diffraction angle, and β is the full width at half maximum (FWHM). Based on the calculations, the crystallite sizes of graphene oxide and $FeCl_3$ nanoparticles were found to be 25.956 ± 0.04 nm and 70.18 ± 0.08 nm, respectively.

Nanoaprticles added ternary fuel blends Preparation

In this study, a ternary fuel blend (D70B20E10) was produced with a volume ratio of 70% conventional diesel, 20% *M. longifolia* biodiesel and 10% ethanol. Hybrid nanoparticles, consisting of $FeCl_3$ and graphene, were added at concentrations of 50 mg/L and 75 mg/L, respectively. The hybrid nanoparticles were divided into two groups: one group was mixed with hexane alone, while the other group was combined with equal proportions of a surfactant and a dispersant together with hexane. The mixtures were sonicated for 35 min at a constant temperature of 35 °C in an ultrasonic bath and then dried to remove the solvent (hexane). After drying, the hybrid nanofuel was prepared by mixing the ternary fuel mixture with the sonicated hybrid nanoparticles. The procedure was carried out with each sample for 20 min at a frequency of 30 kHz. The nanofuel samples used for the analysis are: D70B20E10NPs50 mg/L, D70B20E10NPs75mg/L,D70B20E10NPs50CTAB50mg/L, D70B20E10NPs75CTAB75 mg/L, D70B20E10NPs50QPAN50 mg/L, and D70B20E10NPs75QPAN75 mg/L.

Stability analysis

The increased stability of nanoparticles in liquid fuels can be attributed to their ability to improve combustion properties and promote even combustion of the fuel. However, the introduction of nanoparticles into liquid fuels can lead to the formation of deposits and clogging. Proper dispersion ensures the separation of nanoparticles and prevents their deposition at the bottom of the tank. In this study, ternary fuel blends (D70B20E10) with hybrid nanoparticles were prepared both with and without the addition of dispersants and surfactants. UV spectroscopy was used to evaluate the stability of the nanoparticles by measuring the light transmittance in the wavelength range of 200–1100 nm. Figures 3(a)-(b) show the change in light transmission with wavelength for different fuel samples over two different time intervals.

The stability of the nanofuel samples was evaluated at two specific time intervals, on the 7th and 14th day. A decrease in transmittance indicates an improved stability of the hybrid nanoparticles in the mixture D70B20E10. The inherent haze of the nanoparticles results from their ability to obstruct the light transmittance of the fuel sample. Therefore, a reduction in transmitted light intensity indicates improved stability and dispersion of the nanoparticles. To further improve stability, QPAN and CTAB were added to the hybrid nanoparticles as dispersants. The nanoparticles exhibited effective dispersion, resulting in significant entrapment in the B20 mixture. Since QPAN acts as a dispersant that prevents the agglomeration of nanoparticles by reducing the cohesive forces between the particles. It enhances the repulsive forces between the nanoparticles, resulting in improved separation and uniform dispersion within the fuel matrix. This homogeneous distribution reduces sedimentation at the bottom of the tank and increases the stability of the nanoparticles over a longer period of time. In addition, CTAB is a cationic surfactant that forms a protective layer around the nanoparticles, reducing their surface energy and preventing aggregation. This modification improves the dispersion of the nanoparticles in the liquid fuel. It also promotes better interaction between the nanoparticles and the fuel, improving the overall stability of the nanofuel mixture. Of the samples tested, the fuel combination D70B20E10NPs75QPAN75 mg/L in conjunction with an equal dosage of dispersant (75 mg/L) exhibited the lowest transmittance, indicating superior stability. However, an increase in transmittance was observed on day 14, which was due to the gradual increase in nanoparticle deposition. In addition, the fuel samples were subjected to physicochemical analysis in according to the ATSM standards (see Table 2).

Experimental setup

The four 4-stroke research diesel engine was used for the experimental analysis. The engine operates with greater ease due to a phenomenon known as eddy current loading. The technical data are listed in Table 3, while the schematic diagram of the test setup is shown in Fig. 4. A performance evaluation was carried out by analysing the fuel consumption time. In addition, a MARS gas analyzer was used to measure gaseous emissions such as CO, UHC, and NO_x. The gas analyzer uses advanced non-dispersive infrared

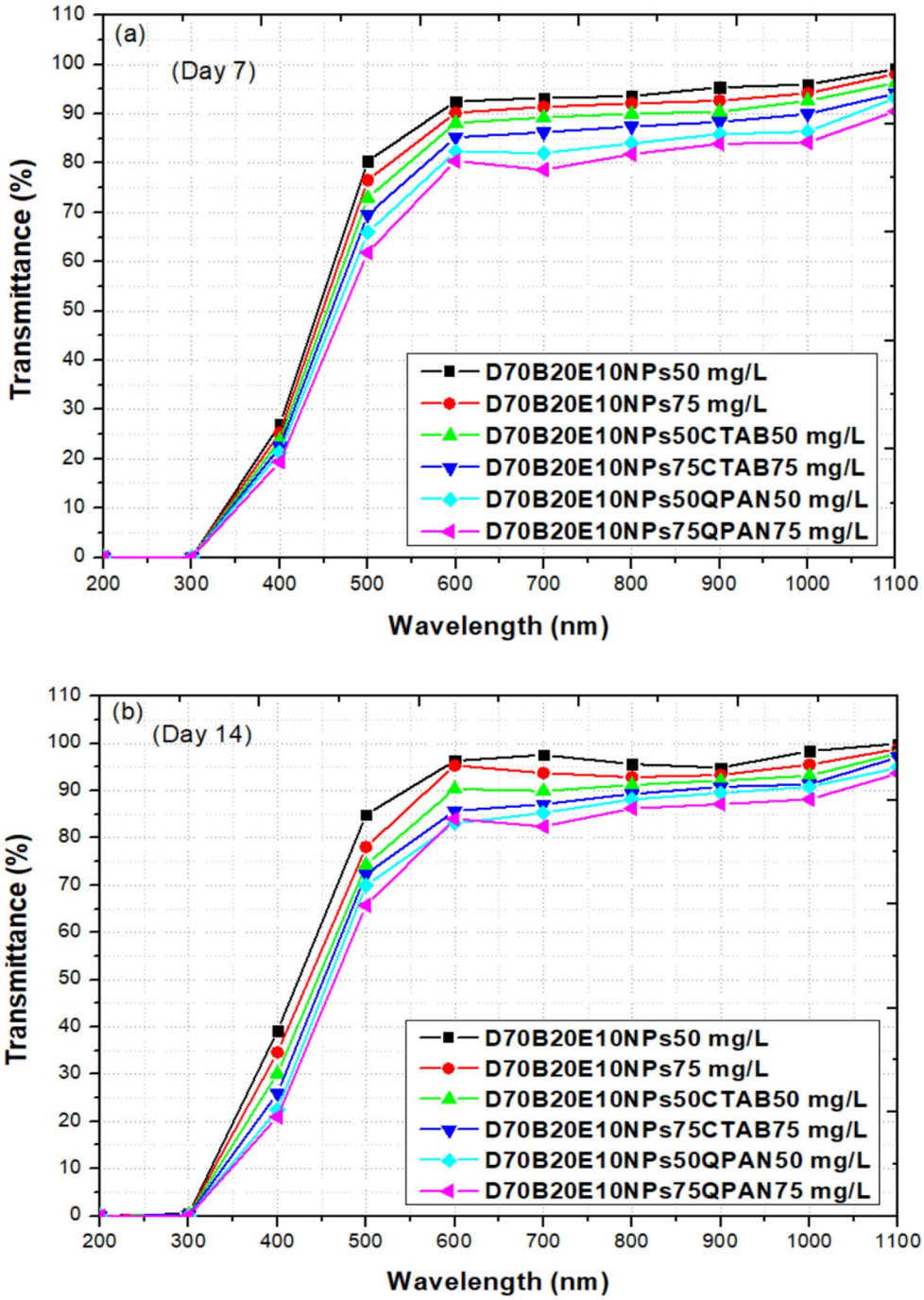

Fig. 3 Stability of nanoparticles at **(a)** Day 7 **(b)** Day 14

technology for CO and UHC measurement, while chemiluminescence detection was used for precise NO_x quantification. For smoke opacity measurement, a MARS smoke meter based on the principle of optical light absorption was used to determine smoke density. To ensure accuracy and consistency, all emission meters were regularly calibrated before and after the tests. All sensors related to the operating parameters were connected to the computer via the data acquisition system.

The tests were carried out for 20 min under steady-state operating conditions, with no preload applied. Performance and emissions data were then recorded at various load levels (3, 6, 9, and 12 kgf) and injection pressures (200, 225 and 250 bar), while maintaining a constant engine speed of 1500 rpm. By testing different pressure levels, the effects of different operating conditions could be thoroughly evaluated, while the selection of specific fuel proportions allowed a detailed investigation of the synergistic effects between fuel properties and engine behaviour. The selected injection

Table 2 Properties of fuel samples

Fuel property	Density (kg/m^3)	Kinematic viscosity (cSt)	Cetane index	Heating value (kJ/kg)
Method	ASTMD1298	ASTMD445	ASTMD976	ASTMD4809
ASTM range	860–900	2.5-6	48 (min)	42,000
D100	839	3.2	52	42,936
D70B20E10	878	3.82	57	41,233
D70B20E10NPs50 mg/L	880	3.88	58	42,981
D70B20E10NPs75 mg/L	882	3.89	58	43,028
D70B20E10NPs50CTAB50 mg/L	884	3.91	59	43,449
D70B20E10NPs75CTAB75 mg/L	884	3.93	60	43,672
D70B20E10NPs50QPAN50 mg/L	887	3.96	60	43,855
D70B20E10NPs75QPAN75 mg/L	889	3.98	61	43,905

Table 3 Specifications of the experimental setup

Constraint	Details
BP (kW) and Make	3.5 and Kirloskar
Speed (RPM)	1500
Engine load (kgf)	3, 6, 9, and 12
Injection pressure (bar)	200, 225, and 250
Number of cylinders	Single
Compression ratio	17.5
Bore (mm)	87.5
Stroke (mm)	110

pressure range of 200 bar to 250 bar kept the pressures within the parameters of normal diesel injection systems, preventing excessive wear of the injectors. Higher injection pressures improve atomization of high viscosity fuels, such as biodiesel blends, provide better air-fuel mixing and reduce incomplete combustion. The tests also included conventional diesel fuel, followed by B20 and ternary fuel blends with nano-fuel as a base. To ensure accuracy, multiple measurements were taken at each test point and the results were averaged to minimise random error. Error bars representing the standard deviation were added to the graphs for clarity and reliability. The BTE measures the effectiveness of converting the chemical energy of the fuel into usable mechanical energy at the engine output shaft, while the BSFC measures the fuel consumption per unit of brake power generated. The BTE and BSFC were calculated using the following Eqs. (2) and (3):

$$BTE = \frac{BP}{(tfc \times CV)} \tag{2}$$

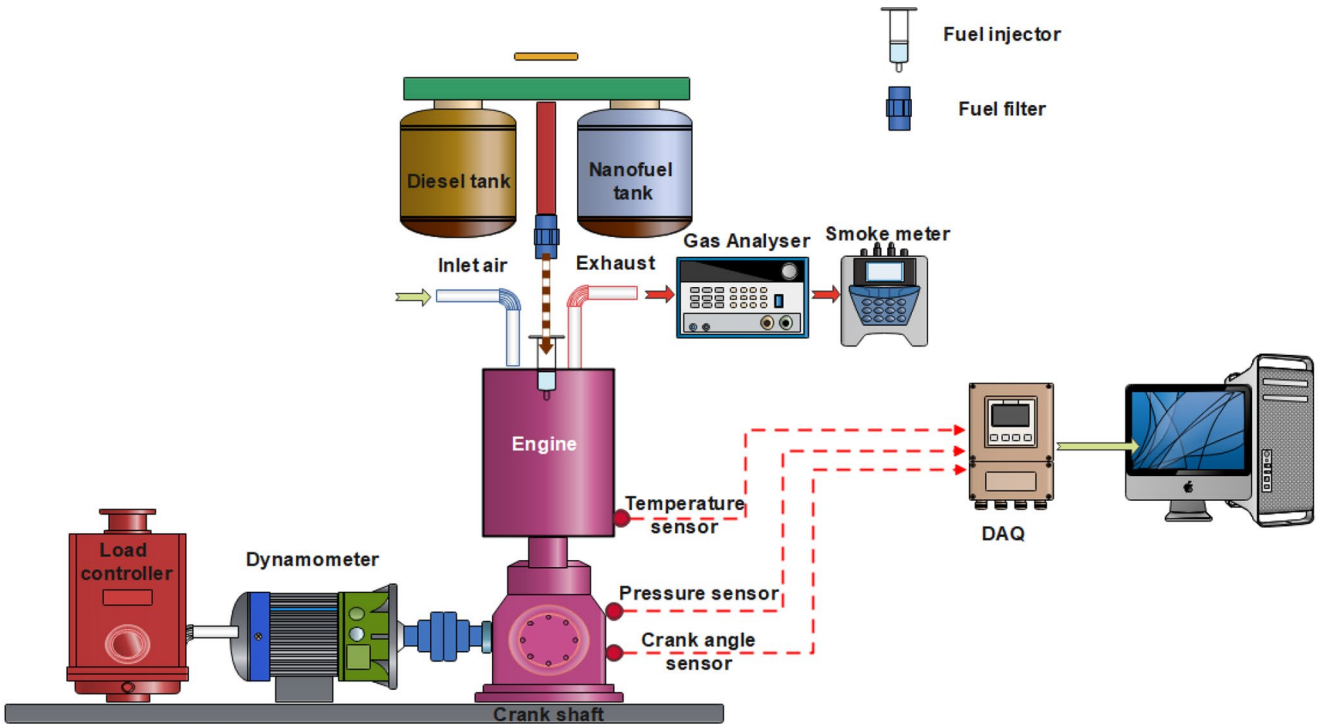

Fig. 4 Pictorial representation of experimental setup

$$BSFC = \frac{tfc}{BP} \quad (3)$$

Where,

$$tfc = \frac{\{V_f \times (BD \times \rho_{biodiesel} + D \times \rho_{diesel}) \times 3600\}}{t \times 10^6},$$

$$BP = \frac{2\pi \times N \times W \times L}{60000}, kW$$

Where the BTE is brake thermal efficiency, BP denotes brake power (kW), tfc is total fuel consumption, BSFC is brake specific fuel consumption, V_f is Volume (m^3), $\rho_{biodiesel}$ = Density of biodiesel (kg/m^3), ρ_{diesel} = Density of diesel (kg/m^3), t is Time (seconds), BD is quantity of biodiesel in %, D is quantity diesel in %, N is the speed in rpm, W is the weight in kg and L is the arm length in metres.

Results and discussion

Performance characteristics

BTE

The variations in BTE as a function of load at different injection pressures are shown in Fig. 5(a)-(c). It has been shown that lower fuel atomization and shorter ignition delay lead to a lower BTE of D70B20E10 than that of conventional diesel [16, 20, 21, 25]. The BTE is significantly increased when hybrid nanoparticles are added to D70B20E10 together with surfactants and dispersants. This is due to the phenomenon of micro-explosions and the higher thermal conductivity of the nanoparticles. The addition of nanoparticles improved the combustion process by increasing the thermal conductivity and catalyzing the oxidation of the fuel, resulting in a more complete and efficient combustion process. In addition, the presence of ethanol in the ternary mixture decreased viscosity and improved atomization, which also contributed to better combustion [26–28]. The improved BTE is the result of the more efficient utilization of the fuel's chemical energy, enabled by the higher surface-to-volume ratio of the nanoparticles compared to conventional diesel-biodiesel blends [25, 29–31]. Since higher cylinder pressures and temperatures can lead to lower heat losses to the surrounding components and coolant, the BTE was also increased with increasing load. The energy converted into productive power corresponds to these heat losses [25, 32]. As the injection pressure was increased, the BTE improved significantly. This can be attributed to improved fuel atomization and faster evaporation. The formation of smaller fuel droplets increases the surface area available for combustion, which leads to better fuel-air mixing. This improved atomization enables a more complete and efficient combustion process [30, 33, 34].

At full load and 250 bar, the BTE of D100, D70B20E10, D70B20E10NPs50 mg/L, D70B20E10NPs75 mg/L, D70B20E10NPs50mg/LCTAB50mg/L,D70B20E10NPs75 mg/L CTAB 75 mg/L, D70B20E10NPs50 mg/L QPAN50 mg/L, D70B20E10NPs75 mg/L QPAN75 mg/L are 26.98%, 26.08%, 28.79%, 31.26%, 31.98%, 33.14%, and 33.26%, respectively. With a higher BTE of 33.26% among all is D70B20E10NPs75 mg/L QPAN75 mg/L.

BSFC

The BSFC is shown in Fig. 6(a)-(c) as a function of load and injection pressure. It can be observed that the BSFC is higher with D70B20E10 than with normal diesel. This is explained by the higher kinematic viscosity of D70B20E10 compared to regular diesel [16, 20, 25, 27] and its lower energy content. The addition of hybrid nanoparticles to the D70B20E10 fuel blend resulted in a greater reduction in BSFC compared to conventional diesel fuel. This improvement can be attributed to the improved fuel properties, particularly the increased heating value, which promotes more efficient and energy-rich combustion by producing high-quality fuel droplets upon atomization [26, 35, 36]. In addition, the higher surface-to-volume ratio of the nanoparticles and better thermal conductivity enable better heat transfer and combustion kinetics, which contributes to lower fuel consumption. The use of dispersants and surfactants, such as QPAN and CTAB, improved the stability of the hybrid nanoparticles in the fuel. This improved stability provided uniform dispersion, resulting in more complete combustion and a significant reduction in the BSFC of the biodiesel blend [30–31, 37]. At higher loads, higher cylinder pressures and temperatures improved the combustion of the fuel-air mixture, resulting in a decrease in BSFC. This decrease can be attributed to higher combustion efficiency, which allows higher energy recovery from each unit of fuel consumed [25, 27–32]. In addition, the increase in injection pressure led to a further decrease in BSFC due to improved atomization, which increased combustion efficiency while minimizing heat rejection. Ultimately, the lower BSFC reflects a more efficient conversion of fuel energy into useful work achieved by reducing heat losses during the combustion process [30, 33, 34].

At 250 bar injection pressure and full load, the BSFC of D100, D70B20E10, D70B20E10NPs50 mg/L, D70B20E10NPs75 mg/L, D70B20E10NPs50 mg/L CTAB 50 mg/L, D70B20E10NPs75 mg/L CTAB 75 mg/L, D70B20E10NPs50 mg/L QPAN50 mg/L, D70B20E10NPs75 mg/L QPAN75 mg/L were 0.223 kg/

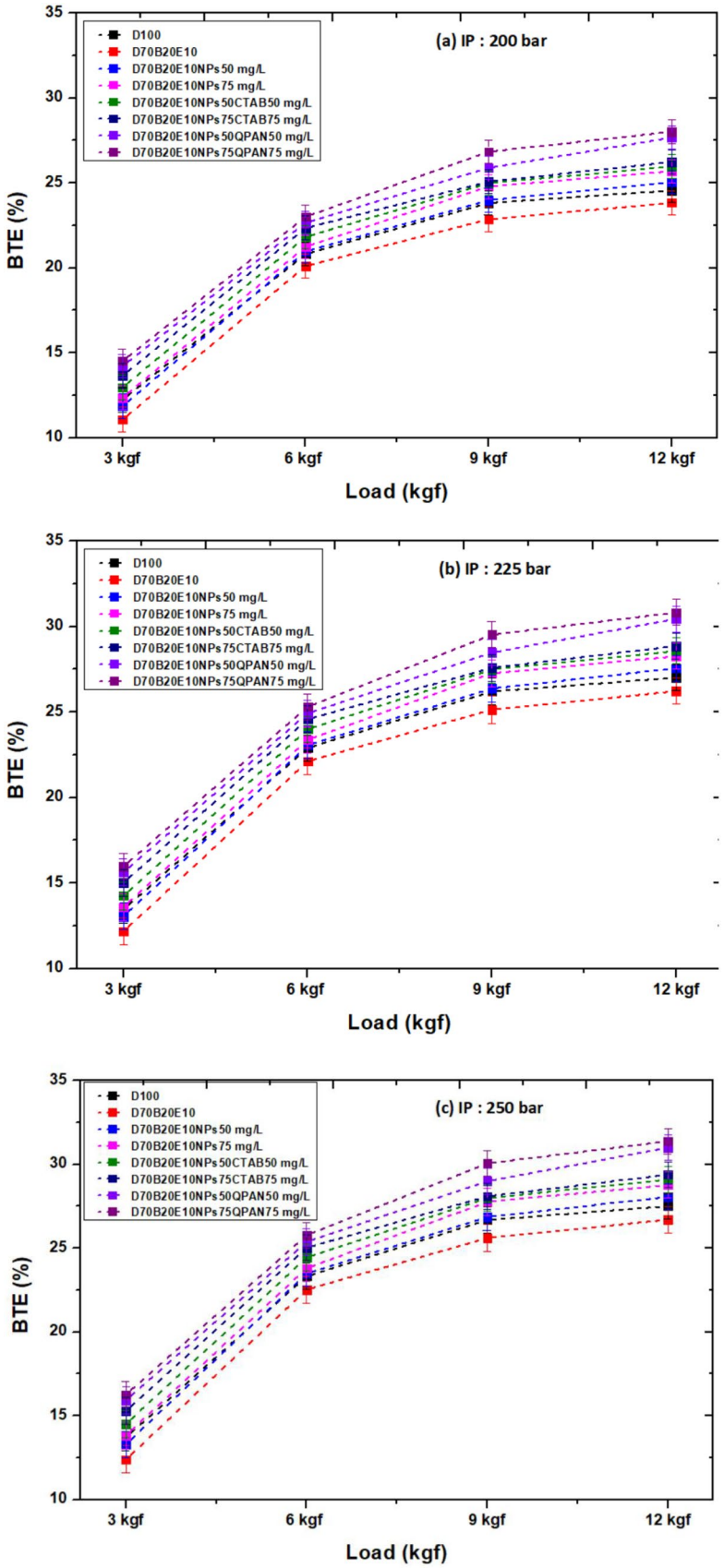

Fig. 5 **(a)-(c)** BTE against load for different injection pressures

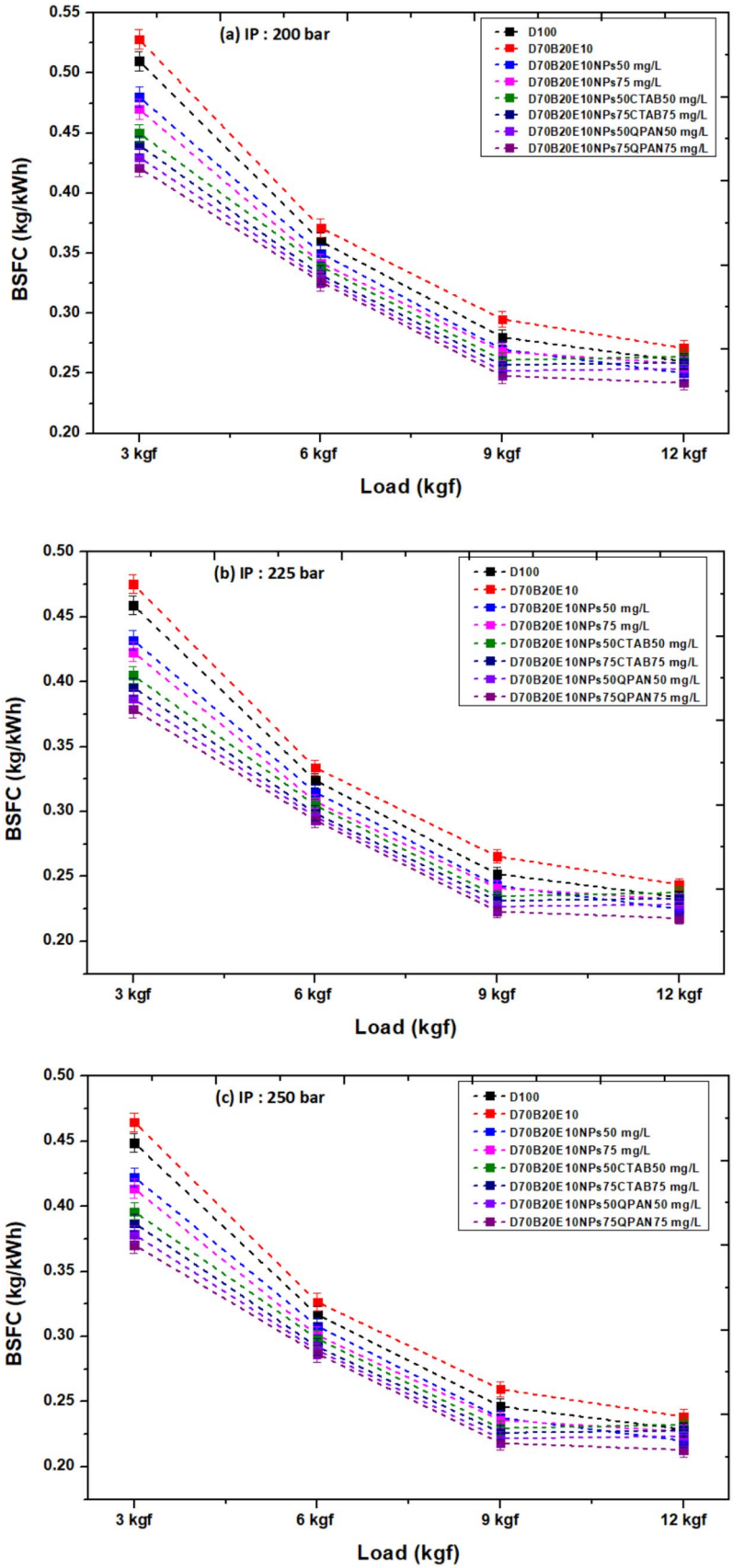

Fig. 6 **(a)-(c)** BSFC against load at different injection pressures

kWh, 0.235 kg/kWh, 0.222 kg/kWh, 0.222 kg/kWh, 0.217 kg/kWh, 0.224 kg/kWh, 0.206 kg/kWh. The lowest BSFC was shown by D70B20E10NPs75 mg/L QPAN75 mg/L.

Emission characteristics

CO

Figures 7(a)–(c) depict the relationship between CO emissions, load, and injection pressure. The use of a ternary fuel blend resulted in lower CO emissions compared to pure diesel, primarily due to the higher oxygen content in biodiesel [20, 21, 24, 25]. This additional oxygen promotes better combustion by facilitating the oxidation of carbon monoxide to carbon dioxide, thus reducing CO emissions. The addition of hybrid nanoparticles to the D70B20E10 fuel blend further contributed to a significant reduction in CO emissions. This improvement can be attributed to the effective dispersion of the nanoparticles, which ensures uniform mixing of the fuel and improves its consistency. The improved homogeneity of the fuel-air mixture leads to more efficient combustion and minimizes the formation of CO as a result of incomplete combustion [14, 33, 34, 36–38]. At higher engine loads, additional fuel is injected into the combustion chamber to cover the increased power requirement. However, if the fuel-air ratio becomes too rich, this can lead to incomplete combustion, resulting in an increase in CO emissions [25, 32]. Finally, higher injection pressures improve the atomization of the fuel into smaller droplets, which improves the fuel-air mixing process and creates a more even and homogeneous mixture in the combustion chamber. This better mixing leads to more efficient and more complete combustion and therefore to a reduction in CO emissions, even at higher loads [30, 33, 34, 39]. At full load and 250 bar injection pressure, the CO of D100, D70B20E10, D70B20E10NPs50 mg/L, D70B20E10NPs75 mg/L, D70B20E10NPs50 mg/L CTAB 50 mg/L, D70B20E10NPs75 mg/L CTAB 75 mg/L, D70B20E10NPs50 mg/L QPAN50 mg/L, D70B20E10NPs75 mg/L QPAN75 mg/L were 0.119%, 0.069%, 0.049%, 0.039%, 0.029%, 0.027%, and 0.019%. In the fuel samples, D70B20E10NPs75 mg/L QPAN75 mg/L has the lowest CO.

UHC

The UHC is shown in Fig. 8(a)–(c) as a function of load and injection pressure. It has been found that the UHC value of the ternary fuel blend is lower compared to regular diesel fuel due to the higher oxygen content [20, 21, 23, 24]. A further reduction in UHC emissions was observed with the addition of hybrid nanoparticles. This is due to the improved combustion process, which provides a larger surface area for fuel and air mixing, allowing for better and more complete combustion. The larger surface-to-volume ratio of the nanoparticles allows for a finer distribution of fuel droplets, resulting in a more even and thorough combustion. This reduces the number of unburned hydrocarbons in the exhaust gas as more of the fuel is fully oxidized during the combustion process [14, 15, 38]. At higher loads, the fuel-air ratio can become richer, which increases the likelihood of incomplete combustion and thus leads to an increase in UHC [25, 32]. Finally, increasing the injection pressure can effectively reduce UHC through better atomization, resulting in more thorough combustion of the fuel-air mixture [30, 33, 40]. UHC of D100, D70B20E10, D70B20E10NPs50 mg/L, D70B20E10NPs75 mg/L, D70B20E10NPs50 mg/L CTAB 50 mg/L, D70B20E10NPs75 mg/L CTAB 75 mg/L, D70B20E10NPs50 mg/L QPAN50 mg/L, D70B20E10NPs75 mg/L QPAN75 mg/L were 47 ppm, 44 ppm, 40 ppm, 34 ppm, 35 ppm, 30 ppm, 24 ppm, and 21 ppm at full load and an injection pressure of 250 bar. The lowest UHC was achieved with D70B20E10NPs75 mg/L QPAN75 mg/L compared to the other fuel samples.

NO_x

The change in the NO_x value with load and injection pressure is shown in Fig. 9(a)–(c). The NO_x of the ternary fuel blend D70B20E10 produced more NO_x compared to regular diesel because it burns at a higher temperature, has a higher cetane number and contains more oxygen. However, the addition of nanoparticles in D70B20E10 leads to lower NO_x emissions [1, 20, 24]. This reduction is due to a higher convective heat transfer in the combustion chamber, which lowers the average combustion temperature. In addition, the nanoparticles improve catalytic efficiency and effectively remove nitrogen oxides [25, 29, 31, 34, 37]. Higher loads lead to higher NO_x values, as more fuel is fed into the combustion chamber to cover the higher power requirement. Higher combustion temperatures and pressures caused by the combustion of more fuel promote the formation of NO_x [25, 32, 34]. Finally, NO_x emissions increased with rising injection pressure due to improved fuel atomization, which enhanced combustion efficiency and elevated temperatures, resulting in higher NO_x formation [30, 33, 34, 40]. At 250 bar, the NO_x of D100, D70B20E10, D70B20E10NPs50 mg/L, D70B20E10NPs75 mg/L, D70B20E10NPs50 mg/L CTAB 50 mg/L, D70B20E10NPs75 mg/L CTAB 75 mg/L, D70B20E10NPs50 mg/L QPAN50 mg/L, D70B20E10NPs75 mg/L QPAN75 mg/L were 1126 ppm, 1193 ppm, 1069 ppm, 952 ppm, 916 ppm, 894 ppm, 862 ppm and 833 ppm, respectively.

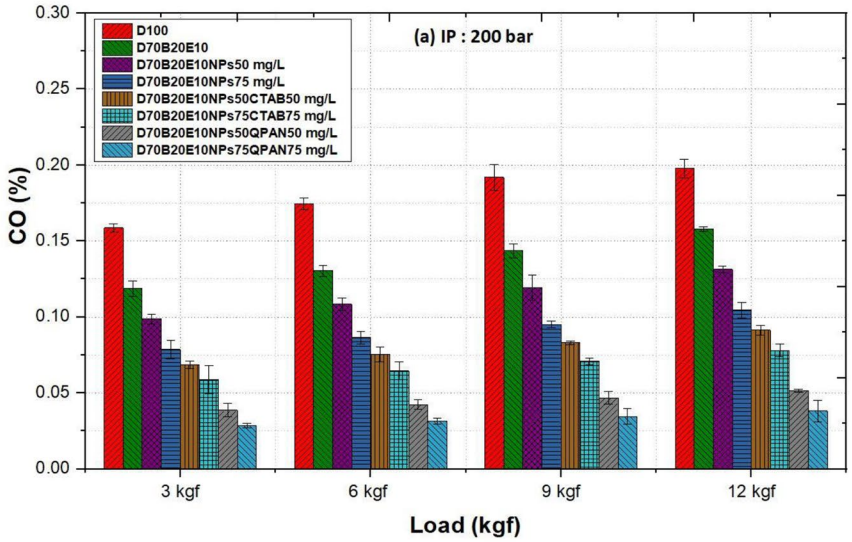

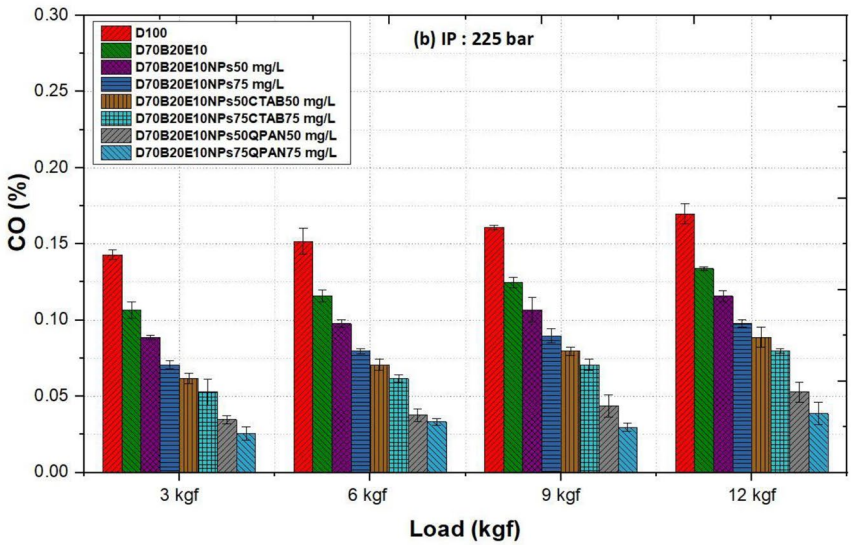

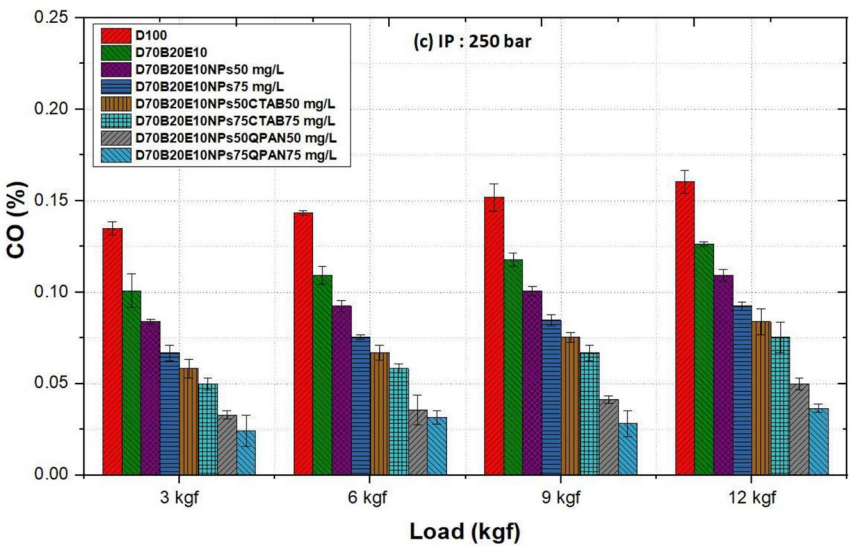

Fig. 7 **(a)-(c)** CO against load at different injection pressures

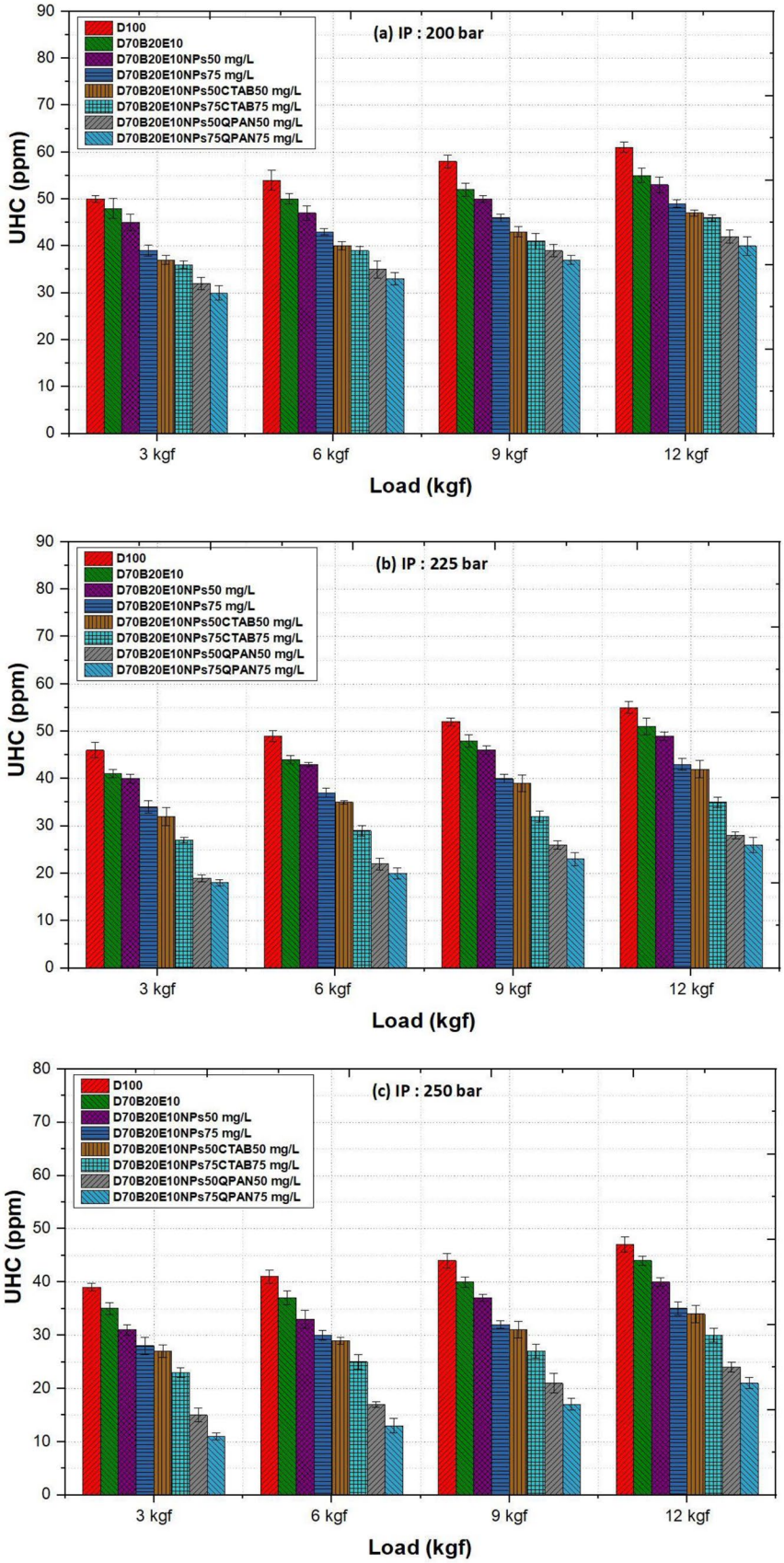

Fig. 8 **(a)-(c)** UHC against load at different injection pressures

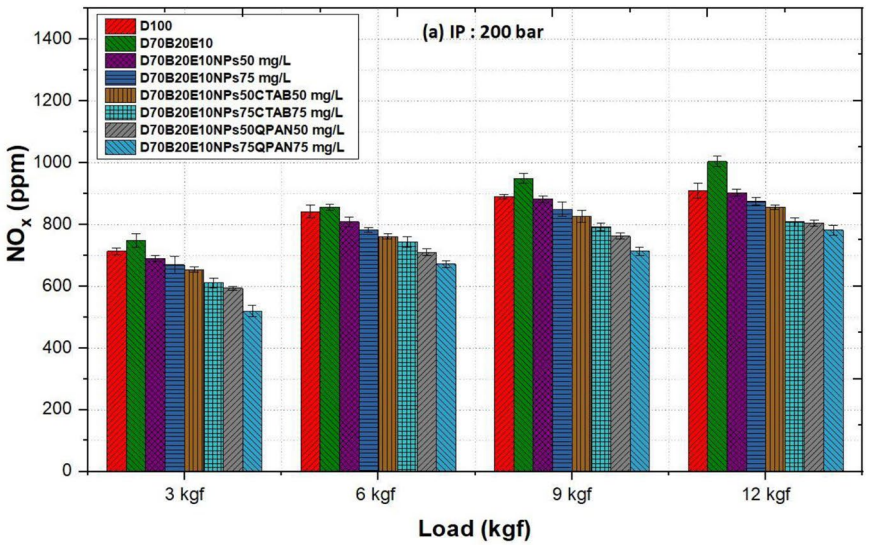

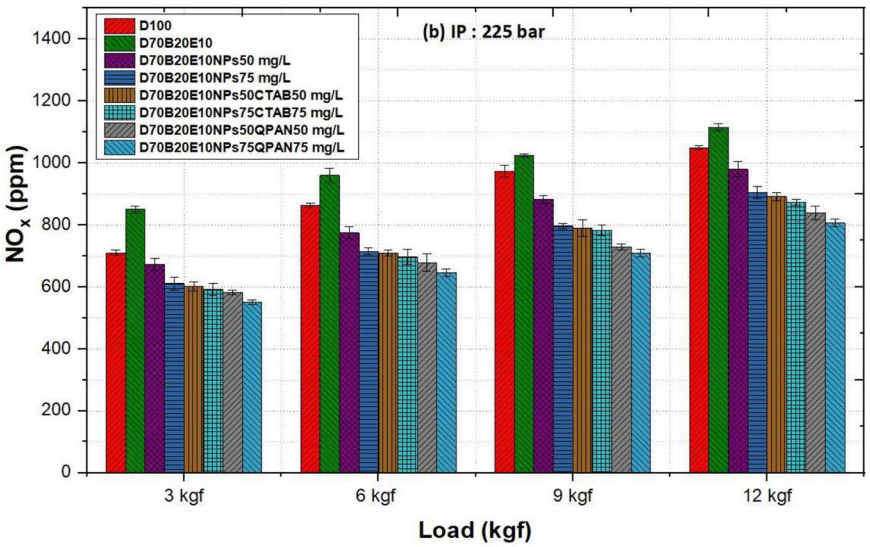

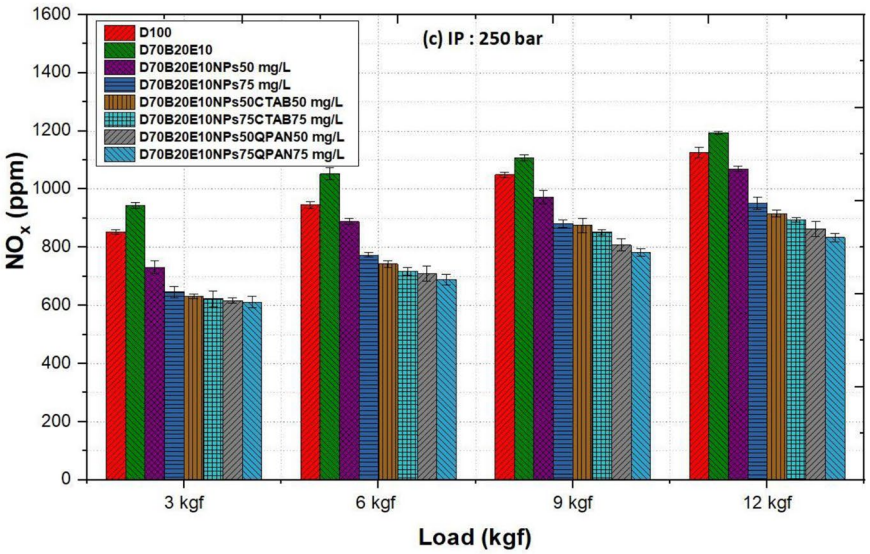

Fig. 9 **(a)-(c)** NO_x against load at different injection pressures

Smoke opacity

The smoke opacity as a function of the load and the injection pressure is shown in Fig. 10(a)–(c). It was found that the smoke opacity of the ternary fuel blend (D70B20E10) was reduced compared to normal diesel fuel due to the higher oxygen content [1, 25, 32]. When nanoparticles were dispersed in D70B20E10, a further reduction in smoke opacity was observed compared to diesel and ternary fuel blends. This was due to the fact that a higher surface area to volume ratio, which increases the ignition properties of the fuel samples [14, 15, 25, 32]. In addition, the smoke opacity showed an increasing tendency with load, which is due to higher temperatures and pressures during combustion, which increase with increasing engine load [25, 32]. Finally, the smoke opacity decreased with increasing injection pressure. This is because the fuel is atomized more finely, which means that more fuel comes into contact with oxygen during combustion [30, 33]. The smoke opacity of D100, D70B20E10, D70B20E10NPs50 mg/L, D70B20E10NPs75 mg/L, D70B20E10NPs50 mg/L CTAB 50 mg/L, D70B20E10NPs75 mg/L CTAB 75 mg/L, D70B20E10NPs50 mg/L QPAN50 mg/L, D70B20E10NPs75 mg/L QPAN75 mg/L were 47.94%, 46.09%, 44.53%, 41.53%, 41.14%, 39.94%, 37.49%, and 36.25%, respectively. At full load and 250 bar, D70B20E10NPs75 mg/L QPAN75 mg/L produced the lowest smoke value.

Conclusions

The performance and emissions of a diesel engine employing a combination of ternary fuel blends of *M. longifolia* biodiesel/diesel/ethanol and $FeCl_3$ and graphene hybrid nanoparticles were examined in this work. From this analysis, the following findings were made:

- The stability of a nanofuel based on D70B20E10 was significantly increased by the addition of dispersant and surfactant. D70B20E10NPs75QPAN75 mg/L showed the highest stability of all fuel samples. In addition, the physicochemical properties of the ternary fuel blend were improved by the addition of nanoparticles and accomplish the ASTM standards.
- Compared to diesel, D70B20E10 performs poorly; however, the hybrid nanoparticles perform better. The maximum BTE for D70B20E10NPs75QPAN75 mg/L was 33.26% at peak load and 250 bar injection pressure; the lowest BSFC was 0.206 kg/kWh.
- When hybrid nanoparticles were added to D70B20E10, emissions fell significantly compared to normal diesel fuel. Furthermore, of all the fuels tested, the one with a concentration of D70B20E10NPs75QPAN75 mg/L showed the lowest reduction in emissions.
- The lower CO, UHC, NO_x, and smoke emissions for D70B20E10NPs75QPAN75 mg/L were 0.019%, 21 ppm, 833 ppm, and 36.25% respectively at maximum load and 250 bar injection pressure.

The results show that the addition of dispersants to nanofuel promotes complete combustion of the fuel and thus reduces engine exhaust emissions. It is recommended to use hybrid nanoparticles in a direct injection diesel engine fuelled with a combination of *M. longifolia* biodiesel, diesel and ethanol without additional modifications to improve engine performance in conjunction with a surfactant and dispersant.

The results of this study can form the basis for further developments in the creation of alternative fuels and research into the possibilities of more environmentally friendly diesel engine technology. The long- term sustainability of the transportation industry could be improved by these developments.

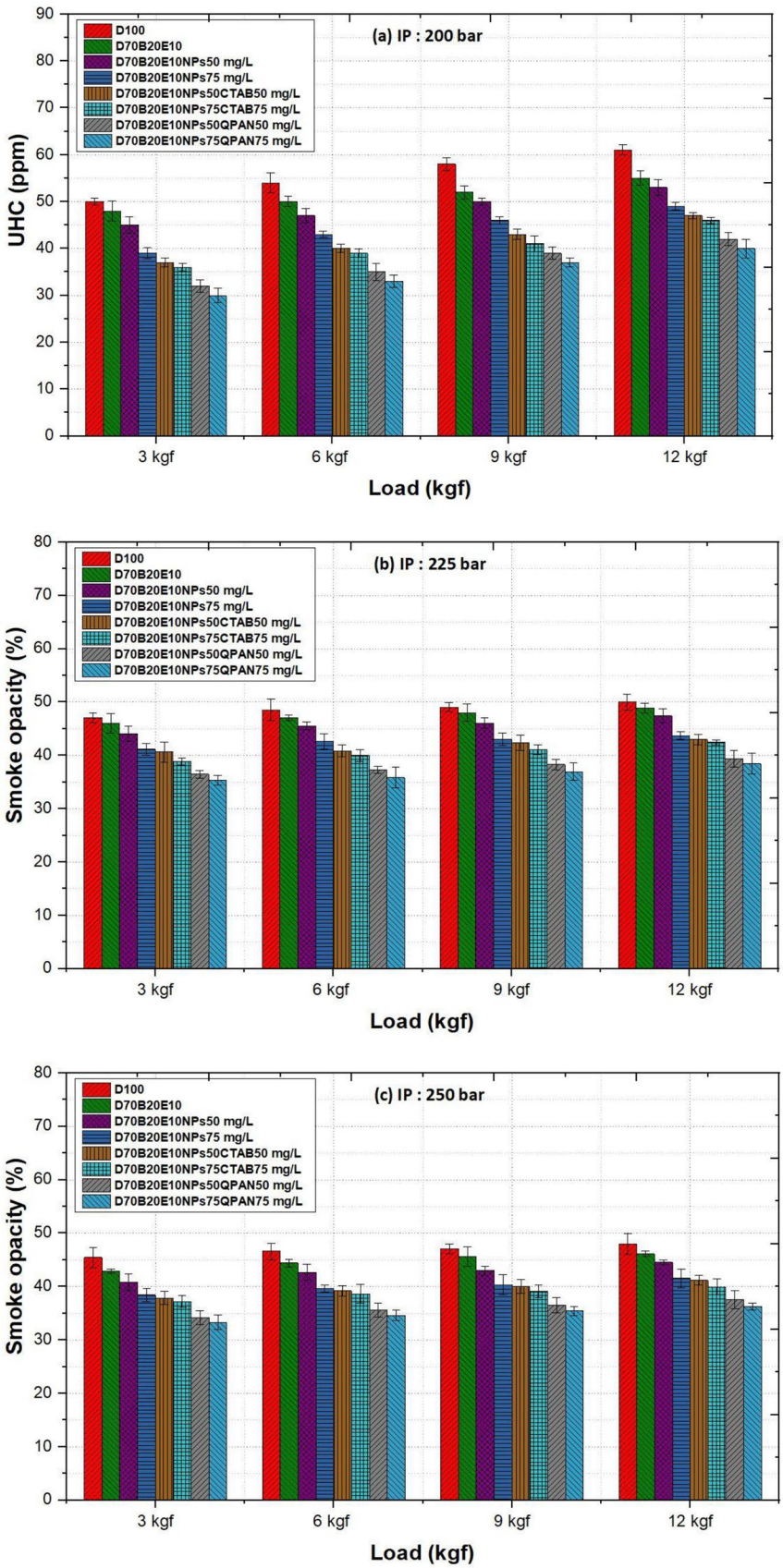

Fig. 10 **(a)-(c)** Smoke opacity against load at different injection pressures

Data availability Not applicable.

Declarations

Conflict of interest No.

References

1. Jaikumar S, Bhatti SK, Srinivas V (2019) Experimental investigations on performance, combustion, and emission characteristics of Niger (*Guizotia abyssinica*) seed oil Methyl ester blends with diesel at different compression ratios. Arab J Sci Eng 44:5263–5273. https://doi.org/10.1007/s13369-018-3538-y
2. Siddique MF, Selim MYE, Elgendi M, Ghannam MT (2024) A review on slurry-based fuels for engines and furnaces: preparation, stability, emission characteristics and application. Int J Thermofluids 22:100610. https://doi.org/10.1016/j.ijft.2024.100610
3. Reddy VL, Sagari J, Vadapalli S, Prasad VVS (2023) Application of response surface methodology to the operating parameters of diesel engines fueled with SiO2 nanoparticles in Abrus precatorius biodiesel. Emergent Mater 6(4):1177–1192. https://doi.org/10.1007/s42247-023-00521-z
4. Mohan K, Sathishkumar P, Rajan DK, Rajarajeswaran J, Ganesan AR (2023) Black soldier fly (Hermetia illucens) larvae as potential feedstock for the biodiesel production: recent advances and challenges. Sci Total Environ 859:160235. https://doi.org/10.1016/j.scitotenv.2022.160235
5. Jaikumar S, Bhatti SK, Srinivas V, Satyameher R, Padal SB, Chandravathi D (2022) Combustion, vibration, and noise characteristics of direct injection VCR diesel engine fuelled with mesua Ferrea oil Methyl ester blends. Int J Ambient Energy 43(1):1569–1580. https://doi.org/10.1080/01430750.2020.1713888
6. Madihi R, Pourfallah M, Gholinia M, Armin M, Ghadi AZ (2022) Thermofluids analysis of combustion, emissions, and energy in a biodiesel ($C_{11}H_{22}O_2$)/natural gas heavy-duty engine with RCCI mode (Part II: fuel injection time/fuel injection rate). Int J Thermofluids 16:100200. https://doi.org/10.1016/j.ijft.2022.100200
7. Ashokkumar V, Salam Z, Sathishkumar P, Hadibarata T, Yusoff ARM, Ani FN (2015) Exploration of fast growing Botryococcus sudeticus for upstream and downstream process in sustainable biofuels production. J Clean Prod 92:162–167. https://doi.org/10.1016/j.jclepro.2015.01.004
8. Sekoai PT, Ouma CNM, Du Preez SP, Modisha P, Engelbrecht N, Bessarabov DG, Ghimire A (2019) Application of nanoparticles in biofuels: an overview. Fuel 237:380–397. https://doi.org/10.1016/j.fuel.2018.10.030
9. Bacha HB, Ullah N, Hamid A, Shah NA (2024) A comprehensive review on nanofluids: synthesis, cutting-edge applications, and future prospects. Int J Thermo Fluids 22:100595. https://doi.org/10.1016/j.ijft.2024.100595
10. Djermouni M, Ouadha A (2023) Thermodynamic analysis of methanol, ammonia, and hydrogen as alternative fuels in HCCI engines. Int J Thermo Fluids 19:100372. https://doi.org/10.1016/j.ijft.2023.100372
11. Mohite A, Bora BJ, Ağbulut Ü, Sharma P, Medhi BJ, Barik D (2024) Optimization of the pilot fuel injection and engine load for an algae biodiesel-hydrogen run dual fuel diesel engine using response surface methodology. Fuel 357:129841. https://doi.org/10.1016/j.fuel.2023.129841
12. Arslan E, Atelge MR, Kahraman N, Ünalan S, Çeper BA (2024) Examination of the effect on the engine of diesel-nanoparticle mixture with natural gas addition. Fuel 357:129911. https://doi.org/10.1016/j.fuel.2023.129911
13. Simhadri K, Rao PS, Paswan M (2024) Improving the combustion and emission performance of a diesel engine with TiO_2 nanoparticle blended Mahua biodiesel at different injection pressures. Int J Thermofluids 21:100563. https://doi.org/10.1016/j.ijft.2024.100563
14. Garugubilli R, Prasad VVS, Sagari J (2024) Experimental investigation on diesel engine operating with CuO nanoparticles dispersed *Azadirachta indica* biodiesel. Int J Thermofluids 22:100641. https://doi.org/10.1016/j.ijft.2024.100641
15. Kunchi LR, Bhatti SK, Lankapalli SVP, Sagari J (2024) Effect of multi ferrites nanoparticles added Terminalia bellirica biodiesel on diesel engine: combustion, performance, and emission studies. Int J Thermofluids 22:100652. https://doi.org/10.1016/j.ijft.2024.100652
16. Kari J, Vanthala VSP, Sagari J (2024) Performance and emission characteristics of a diesel engine fuelled with mesua Ferrea biodiesel with chromium oxide (Cr_2O_3) nanoparticles: experimental approach and response surface methodology. Int J Thermofluids 22:100637. https://doi.org/10.1016/j.ijft.2024.100637
17. Ansari AM, Memon LA, Ghannam MT, Selim MY (2023) Impact of biodiesel blended fuel with nanoparticles on performance and noise emission in compression ignition engine. Int J Thermofluids 19:100390. https://doi.org/10.1016/j.ijft.2023.100390
18. Janakiraman S, Lakshmanan T, Raghu P (2021) Experimental investigative analysis of ternary (diesel + biodiesel + bio-ethanol) fuel blended with metal-doped titanium oxide nanoadditives tested on a diesel engine. Energy 235:121148. https://doi.org/10.1016/j.energy.2021.121148
19. El-Seesy AI, Nour M, Attia AM, He Z, Hassan H (2020) Investigation the effect of adding graphene oxide into diesel/higher alcohols blends on a diesel engine performance. Int J Green Energy 17(3):233–253. https://doi.org/10.1080/15435075.2020.1722132
20. Nutakki PK, Gugulothu SK, Ramachander J, Sivasurya M (2022) Effect of n-amyl alcohol/biodiesel blended nano additives on the performance, combustion and emission characteristics of CRDi diesel engine. Environ Sci Pollut Res 29:82–97. https://doi.org/10.1007/s11356-021-13165-5
21. Yesilyurt MK, Yilbasi Z, Aydin M (2020) The performance, emissions, and combustion characteristics of an unmodified diesel engine running on the ternary blends of Pentanol/safflower oil biodiesel/diesel fuel. J Therm Anal Calorim 140:2903–2942. https://doi.org/10.1007/s10973-020-09376-6
22. Preuß J, Munch K, Denbratt I (2018) Performance and emissions of long-chain alcohols as drop-in fuels for heavy duty compression ignition engines. Fuel 216:890–897. https://doi.org/10.1016/j.fuel.2017.11.122
23. Yilmaz N, Atmanli A, Vigil FM (2018) Quaternary blends of diesel, biodiesel, higher alcohols and vegetable oil in a compression ignition engine. Fuel 212:462–469. https://doi.org/10.1016/j.fuel.2017.10.050
24. Mujtaba MA, Kalam MA, Masjuki HH, Gul M, Soudagar MEM, Ong HC, Waqar A, Atabani AE, Razzaq L, Yusoff M (2020) Comparative study of nanoparticles and alcoholic fuel additives-biodiesel-diesel blend for performance and emission improvements. Fuel 279:118434. https://doi.org/10.1016/j.fuel.2020.118434
25. Jaikumar S, Srinivas V, Prasad VVS, Susmitha G, Sravya P, Sajala A, Jaswitha L (2021) Experimental studies on the performance and emission parameters of a direct injection diesel engine fueled with nanoparticle-dispersed biodiesel blend. Nanatechnol Environ Eng 6(15). https://doi.org/10.1007/s41204-021-00113-4
26. Kegl T, Kralj AK, Kegl B, Kegl M (2021) Nanomaterials as fuel additives in diesel engines: A review of current State, opportunities, and challenges. Prog Energy Combust Sci 83:100897. https://doi.org/10.1016/j.pecs.2020.100897
27. El-Seesy AI, Mohamed N, Ali MAA, Zhixia H, Hamdy H (2020) Investigation the effect of adding graphene oxide into diesel/

higher alcohols blends on a diesel engine performance. Int J Green Energy 17(3):233–253. https://doi.org/10.1080/15435075.2020.1722132
28. Srinidhi C, Madhusudhan A, Channapattana SV (2019) Effect of NiO nanoparticles on performance and emission characteristics at various injection timings using biodiesel-diesel blends. Fuel 235:185–193. https://doi.org/10.1016/j.fuel.2018.07.067
29. Pala SR, Vanthala VSP, Sagari J (2023) Influence of graphene oxide nanoparticles dispersed Mahua oil biodiesel on diesel engine: performance, combustion, and emission study. Biofuels 14(10):1027–1036. https://doi.org/10.1080/17597269.2023.2206696
30. Illipilla M, Lankapalli SVP, Sagari J (2023) Experimental study on a diesel engine fueled with *Semecarpus anacardium* biodiesel containing dispersed TiO_2 nanoparticles: performance, combustion, and emission analyses. Energy Ecol Environ 8(2):113–128. https://doi.org/10.1007/s40974-022-00265-2
31. Kari J, Vanthala VSP, Sagari J (2023) The influence of Cr_2O_3 nanoparticles dispersed mesua Ferrea biodiesel on the analysis performance, combustion, and emissions of diesel engine. Environ Dev Sustain 26:4551–4577. https://doi.org/10.1007/s10668-022-02897-0
32. Jaikumar S, Srinivas V, Rajasekhar M (2021) Influence of dispersant added nanoparticle additives with diesel-biodiesel blend on direct injection compression ignition engine: combustion, engine performance, and exhaust emissions approach. Energy 224:120197. https://doi.org/10.1016/j.energy.2021.120197
33. Shariff SH, Vadapalli S, Sagari J (2022) Experimental study on direct injection diesel engine fuelled with ferric chloride nanoparticle dispersed *Cassia Fistula* biodiesel blend. Int J Energy Environ Eng 13(1):179–189. https://doi.org/10.1007/s40095-021-00405-0
34. Reddy VL, Sagari J, Vadapalli S, Prasad VVS (2023) Investigation of operating parameters of diesel engine fueled with SiO_2 nanoparticles and *Abrus precatorius* biodiesel: experimental approach and response surface methodology. Water Air Soil Pollut 234(7):416. https://doi.org/10.1007/s11270-023-06449-8
35. Hoseini SS, Najafi G, Ghobadian B, Mamat R, Ebadi MT, Yusaf T (2018) Novel environmentally friendly fuel: the effects of nanographene oxide additives on the performance and emission characteristics of diesel engines fuelled with *Ailanthus altissima* biodiesel. Renewable Energy 125:283–294. https://doi.org/10.1016/j.renene.2018.02.104
36. Perumal V, Ilangkumaran M (2018) The influence of copper oxide nano particle added pongamia Methyl ester biodiesel on the performance, combustion and emission of a diesel engine. Fuel 232:791–802. https://doi.org/10.1016/j.fuel.2018.04.129
37. Kaki S, Kaur BS, Sagari J (2021) Influence of ZnO nanoparticles and dispersant in Baheda oil biodiesel blend on the assessment of performance, combustion, and emissions of VCR diesel engine. Appl Nanosci 11(11):2689–2702. https://doi.org/10.1007/s13204-021-02233-4
38. EL-Seesy AI, Hamdy H, Ookawar S (2018) Performance, combustion, and emission characteristics of a diesel engine fueled with Jatropha Methyl ester and graphene oxide additives. Energy Conv Manag 166:674–686. https://doi.org/10.1016/j.enconman.2018.04.049
39. Sarıdemir S, Gürel AE, Ağbulut Ü, Bakan F (2020) Investigating the role of fuel injection pressure change on performance characteristics of a DI-CI engine fuelled with Methyl ester. Fuel 271:117634. https://doi.org/10.1016/j.fuel.2020.117634
40. Ağbulut Ü, Ayyıldız M, Sarıdemir S (2020) Prediction of performance, combustion and emission characteristics for a CI engine at varying injection pressures. Energy 197:117257. https://doi.org/10.1016/j.energy.2020.117257